

# Cluster aspects of binary fission

**A V Andreev, G G Adamian and N V Antonenko**

Joint Institute for Nuclear Research, 141980 Dubna, Russia

E-mail: antonenk@theor.jinr.ru

**Abstract.** With the improved scission-point model the mass distributions are calculated for induced fission of different Hg isotopes with even mass numbers  $A = 180, 184, 188, 192, 196, 198$ . The calculated mass distribution and mean total kinetic energy of fission fragments are in a good agreement with the existing experimental data. The change in the shape of the mass distribution from asymmetric to more symmetric is revealed with increasing  $A$  of the fissioning  $^{238}\text{Hg}$  nucleus, and the reactions are proposed to verify this prediction experimentally.

## 1. Introduction

The asymmetric shape of the mass distribution is well known in the spontaneous, neutron induced and  $\beta$ -delayed fission of most actinide isotopes. Such asymmetric shape was theoretically explained by taking into account the shell structure of the fragments [1, 2, 3, 4, 5]. The studies of the Coulomb-excited fission of radioactive nuclei revealed the predominance of symmetric fission in the light thorium to astatine region [6]. In the fission of stable targets with mass numbers  $A = 185 - 210$  induced by protons and  $^3,^4\text{He}$ , the mass distribution was also found to be symmetric in most cases [7]. However, for several nuclei with  $A \approx 200$  the mass distribution looks symmetric, but with a small dip on the top at small excitation energies [7]. Based on the most of experimental data, one could conclude that the asymmetric shape of mass distribution in low-energy fission changes to symmetric one with decreasing mass number of the fissioning nucleus. It was unexpected that in the recent experiment [8] on  $\beta$ -delayed fission of  $^{180}\text{Tl}$  the shape of the mass distribution was found to be clearly asymmetric. The explanation of this interesting result is a challenge for nuclear theory and a good test for the existing models of nuclear fission.

## 2. Cluster approach to the last stage of fission

The statistical scission-point model [1] relies on the assumption that statistical equilibrium is established at scission and the observable characteristics of the fission process are formed near the prescission configurations of the fissioning nucleus. In spite of the criticism raised in more sophisticated models, this model remains to be unique for describing all observable characteristics of fission. With the modified scission-point model [9] we can describe the experimental data on fission of actinides: mass, charge, kinetic energy distributions and neutron multiplicity distributions. With this model a new explanation of a bimodality effect in fission of heavy actinides and fine structure of mass-energy distribution in fission of  $^{236}\text{U}$  have been proposed. The model has also been extended to the description of ternary fission [10].

Here we give a short description of the model [9, 10]. The fissioning nucleus at the scission point is modeled by the two nearly touching coaxial spheroids – fragments of a dinuclear system



with the masses (charges)  $A_L$  ( $Z_L$ ) and  $A_H$  ( $Z_H$ ) of the light ( $L$ ) and heavy ( $H$ ) fragments, respectively.  $A = A_L + A_H$  ( $Z = Z_L + Z_H$ ) is the mass (charge) number of fissioning nucleus. Taking into account the volume conservation, the shape of the system is defined by the mass and charge numbers of the fragments, deformation parameters of the fragments  $\beta_i$  ( $i = L, H$ ) and the interfragment distance  $R$ . The deformation parameter of each fragment is the ratio of the major and minor semi-axes of the spheroid  $\beta_i = c_i/a_i$ . Here and further  $i$  denotes the light or heavy fragments of the dinuclear system. The case  $\beta_i = 1$  corresponds to the spherical shape of the fragment. For small values of  $\beta_i - 1$ , the following equality is valid:  $\beta_i \approx \beta_{2i} + 1$ , where  $\beta_{2i}$  is the parameter of quadrupole deformation of the  $i$ 'th fragment in the multipole expansion of the fragment shape.

The potential energy of the system

$$U(A_i, Z_i, \beta_i, R, l) = U^{macro}(A_i, Z_i, \beta_i, R, l) + \delta U^{shell}(A_i, Z_i, \beta_i), \quad (1)$$

$$\begin{aligned} U^{macro}(A_i, Z_i, \beta_i, R, l) &= U_L^{LD}(A_L, Z_L, \beta_L) + U_H^{LD}(A_H, Z_H, \beta_H) \\ &+ V^C(A_i, Z_i, \beta_i, R) + V^N(A_i, Z_i, \beta_i, R) \\ &+ V^{rot}(A_i, Z_i, \beta_i, R, l) + U^{zpv}(A_i, Z_i), \end{aligned}$$

$$\delta U^{shell}(A_i, Z_i, \beta_i) = \delta U_L^{shell}(A_L, Z_L, \beta_L) + \delta U_H^{shell}(A_H, Z_H, \beta_H)$$

is the sum of the liquid drop energies  $U_i^{LD}$  of each fragment, the energy of interaction of the fragments  $V^C + V^N$ , the rotational energy  $V^{rot}$ , the energy  $U^{zpv}$  of zero-point vibrations, and the shell correction terms  $\delta U_i^{shell}$ . The shell corrections are calculated with the Strutinsky method and two-center shell model [11]; the damping of the shell corrections with excitation energy and angular momentum  $l$  is introduced in our model. The interaction energy consists of the Coulomb interaction  $V^C$  of two uniformly charged spheroids and nuclear interaction  $V^N$  in the form of a double folding of nuclear densities and density-dependent Skyrme-type nucleon-nucleon forces [12]. For  $\beta$ -delayed and induced fission we use zero and non-zero angular momenta  $l$ , respectively (see below). We related the energy  $U^{zpv} = E_i^{2+} \coth[E_i^{2+}/T(l)]$  of zero-point vibrations with the energies  $E_i^{2+}$  of the first  $2^+$  excited states of the fragments from [13]. The definition of the temperature  $T(l)$  is given below. Here, we use a simplification that for all deformations the zero-point vibration energies at zero temperature are equal to the  $E_i^{2+}$  energy at the ground state deformation. However, our calculations show that the nucleus being stiffer in the ground state in comparison to the neighboring nuclei remains stiffer at large deformations. The shape dependence of zero-point vibrations of the nascent fragments is taken effectively into account through the shape dependent temperature or excitation energy. At high excitation energy  $U^{zpv} = T(l)$  for all fragments.

All terms in (1) excepting  $U^{zpv}$  depend on deformations of the fragments. For given deformations of the fragments the interaction potential has a potential minimum (pocket) as a function of the interfragment distance  $R$ . For calculation of the potential energy we take the value of interfragment distance  $R = R_m$  corresponding to this minimum [ $U(A_i, Z_i, \beta_i, l) \equiv U(A_i, Z_i, \beta_i, R_m, l)$ ]. Depending on the masses of the fragments and their deformations the calculated distance between the tips of the spheroids is 0.5–1 fm.

Because the thermodynamical equilibrium is postulated at the scission point, the excitation energy of the nuclear system at scission is calculated as a difference between the potential energy  $U_{CN}(A, Z, \beta, l)$  of the compound nucleus (fissioning nucleus) and the potential energy  $U(A_i, Z_i, \beta_i, l)$  of the dinuclear system at the scission point plus the initial excitation energy  $E_{CN}^*(l)$  of the compound nucleus:  $E^*(l) = U_{CN}(A, Z, \beta, l) - U(A_i, Z_i, \beta_i, l) + E_{CN}^*(l)$ . The temperature is calculated as  $T(l) = \sqrt{E^*(l)/a}$ , where  $a = A/12$  is the level density parameter

in the Fermi-gas model. The yield of a particular scission configuration with given mass and charge numbers and deformation parameters of the fragments is proportional to the exponential Boltzmann-factor:

$$Y(A_i, Z_i, \beta_i, l) \sim \exp \left\{ -\frac{U(A_i, Z_i, \beta_i, l)}{T(l)} \right\}. \quad (2)$$

To obtain the relative mass distribution as a function of the mass number of one of the fragments in fission of a compound nucleus with mass and charge numbers  $A$  and  $Z$ , one should integrate the expression (2) over  $Z_L$ ,  $\beta_L$ , and  $\beta_H$ , sum over  $l$  and take into account that  $A_H = A - A_L$  and  $Z_H = Z - Z_L$ :

$$Y(A_L) = \frac{\sum_{l=0}^{l_{max}} (2l+1) \int \exp \left\{ -\frac{U(A_i, Z_i, \beta_i, l)}{T(l)} \right\} dZ_L d\beta_L d\beta_H}{\sum_{l=0}^{l_{max}} (2l+1) \int \exp \left\{ -\frac{U(A_i, Z_i, \beta_i, l)}{T(l)} \right\} dA_L dZ_L d\beta_L d\beta_H}. \quad (3)$$

The value of angular momentum  $l$  is limited by either the kinetical angular momentum  $l_{kin} = R_b \sqrt{2\mu(E_{c.m.} - V_b)}$  ( $R = R_b$  is the position of the Coulomb barrier with the height  $V_b = V^C(A_i, Z_i, \beta_i = 0, R = R_b) + V^N(A_i, Z_i, \beta_i = 0, R = R_b)$  in the entrance channel,  $\mu = m_0 A_L A_H / (A_L + A_H)$  is the reduced mass parameter, and  $m_0$  is the nucleon mass) or by the calculated critical angular momentum  $l_{cr}$  in the entrance channel, depending on which one is smaller:  $l_{max} = \min\{l_{kin}, l_{cr}\}$ .

We calculate the total kinetic energy (TKE) supposing that all interaction energy at the scission point transforms after fission into the kinetic energy of the fission fragments. Therefore, the value of the TKE strongly depends on the deformation of the fragments at the scission point. The smaller the deformations of the fragments, the larger the Coulomb repulsion, the larger the TKE. The mean value of the total kinetic energy for particular binary splitting is calculated by averaging over deformations of the fragments:

$$\langle TKE \rangle(A_i, Z_i) = \frac{\sum_{l=0}^{l_{max}} (2l+1) \int TKE(A_i, Z_i, \beta_i, l) \exp \left\{ -\frac{U(A_i, Z_i, \beta_i, l)}{T(l)} \right\} d\beta_L d\beta_H}{\sum_{l=0}^{l_{max}} (2l+1) \int \exp \left\{ -\frac{U(A_i, Z_i, \beta_i, l)}{T(l)} \right\} d\beta_L d\beta_H}, \quad (4)$$

where

$$TKE(A_i, Z_i, \beta_i, l) = V^C(A_i, Z_i, \beta_i, R_b) + V^N(A_i, Z_i, \beta_i, R_b) + V_{rel}^{rot}(A_i, Z_i, \beta_i, l), \quad (5)$$

$V_{rel}^{rot}(A_i, Z_i, \beta_i, l) = \hbar^2 f l(f+1) / (2\mu R_b^2)$ ,  $f = \mu R_m^2 / (\mathfrak{I}_L + \mathfrak{I}_H + \mu R_m^2)$ . Here,  $\mathfrak{I}_L$  and  $\mathfrak{I}_H$  denotes the moment of inertia of the fragments.

### 3. Fission of Hg isotopes

For  $\beta$ -delayed fission of  $^{180}\text{Tl}$  [8] the excitation energy  $E_{CN}^*(l=0)$  of the fissioning nucleus  $^{180}\text{Hg}$  does not exceed 10.44 MeV. The mass distribution of fission fragments is presented in fig. 1. We obtained clearly asymmetric mass distribution with the average masses of the light and heavy fragments about 80 and 100, respectively, that is in agreement with the experimental data [8]. The calculated  $\overline{TKE} = 136$  MeV is also in good agreement with the experiment [8].

It is convenient to analyze the obtained results for fission of  $^{180}\text{Hg}$  by comparison of the potential energy surfaces of different mass/charge splits (fig. 2). If one excludes the shell corrections, the potential energy surfaces will have a minimum at the deformations of the

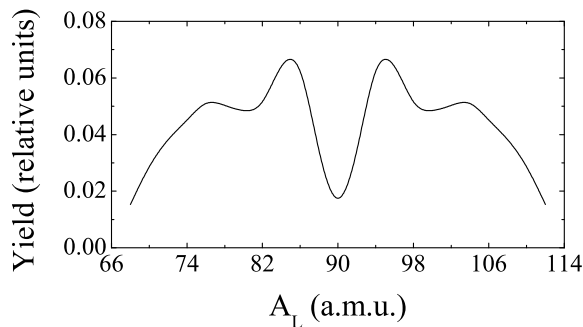


**Figure 1.** Calculated mass distribution of fission fragments for  $\beta$ -delayed fission of  $^{180}\text{Tl}$  (fissioning nucleus is  $^{180}\text{Hg}$ ).

fragments of about  $\beta_i=1.6$ . These  $\beta_i$  are larger than the ground-state deformations of the corresponding nuclei because of the polarization effect. In fission of  $^{180}\text{Hg}$  the symmetric scission configuration is  $^{90}\text{Zr}+^{90}\text{Zr}$ . The shell correction for  $^{90}\text{Zr}$  has a negative value  $\delta U_i^{\text{shell}} \approx -2$  MeV near  $\beta_i=0$ , at larger deformations it becomes positive, at  $\beta_i=1.6$  it is equal to  $\delta U_i^{\text{shell}} \approx 1$  MeV, then grows further and at  $\beta_i=1.85$  reaches  $\delta U_i^{\text{shell}} \approx 4$  MeV. On the contrary, the shell corrections for non-magic nuclei in the scission configurations Kr+Ru and Se+Pd are usually positive at small deformations ( $\delta U_L^{\text{shell}} \approx 2.5$  MeV,  $\delta U_H^{\text{shell}} \approx 1.5$  MeV) and have zero or slightly negative values in the region around  $\beta_i=1.6$ . Because of these shell effects, the minimum is narrow for  $^{90}\text{Zr}+^{90}\text{Zr}$ , while for  $^{76}\text{Se}+^{104}\text{Pd}$ , where the shell effects are weaker, it is wide.

Figure 3 shows a change in the shape of the mass distribution from asymmetric to more symmetric with increasing mass number  $A$  of the fissioning nucleus  $^A\text{Hg}$ . While the mass distribution is well asymmetric for  $^{180}\text{Hg}$  and  $^{184}\text{Hg}$ , for  $^{188}\text{Hg}$  the asymmetry is less pronounced, and for  $^{192}\text{Hg}$  and  $^{196}\text{Hg}$  the mass distribution looks more symmetric but with a dip on the top similar to that observed experimentally in the fission of  $^{198}\text{Hg}$  [7]. In our model, with increasing mass of the fissioning nucleus, the fragments of symmetric scission configurations deviate from the magic  $^{90}\text{Zr}$ , and the role of strong shell effects at symmetric splits decreases. Thereby, in the heavy isotopes of Hg the shape of the mass distribution is generally defined by the liquid-drop part of the energy, and we obtain more symmetric mass distributions.

The excitation energy reduces the shell effects and smooths out the shape of the mass distribution (fig. 3). However, for some isotopes the influence of the excitation energy is rather weak. For example, in the case of  $^{180}\text{Hg}$  the mass distribution has a pronounced asymmetric shape even at the excitation energy  $E_{CN}^*=64.2$  MeV [8].

To study the fission properties of all considered isotopes  $^{180}\text{Hg}$ ,  $^{184}\text{Hg}$ ,  $^{188}\text{Hg}$ ,  $^{192}\text{Hg}$  and  $^{196}\text{Hg}$  (fig. 3), we propose the induced fission reactions at bombarding energies 10 MeV and 30 MeV above the corresponding Coulomb barriers  $V_b$  for the spherical nuclei:  $^{36}\text{Ar}+^{144}\text{Sm} \rightarrow ^{180}\text{Hg}$  ( $V_b=126.2$  MeV,  $l_{\text{max}}=44$  and 61);  $^{40}\text{Ar}+^{144}\text{Sm} \rightarrow ^{184}\text{Hg}$  ( $V_b=124.55$  MeV,  $l_{\text{max}}=46$  and 71);  $^{40}\text{Ar}+^{148}\text{Sm} \rightarrow ^{188}\text{Hg}$  ( $V_b=123.9$  MeV,  $l_{\text{max}}=46$  and 66);  $^{32}\text{S}+^{160}\text{Gd} \rightarrow ^{192}\text{Hg}$  ( $V_b=114.4$  MeV,  $l_{\text{max}}=42$  and 63);  $^{36}\text{S}+^{160}\text{Gd} \rightarrow ^{196}\text{Hg}$  ( $V_b=112.8$  MeV,  $l_{\text{max}}=45$  and 70).

#### 4. Summary

Based on the cluster approach to the last stage of fission, we got a good description of the recent experiment [8] where the asymmetric mass distribution in fission of  $^{180}\text{Hg}$  was observed. The results of our calculations confirm the importance of the shell structure and, correspondingly, the deformation effects in the fission process.

#### Acknowledgments

We thank Dr. A. N. Andreyev for fruitful discussions. This work was supported by DFG (Bonn) and RFBR (Moscow).

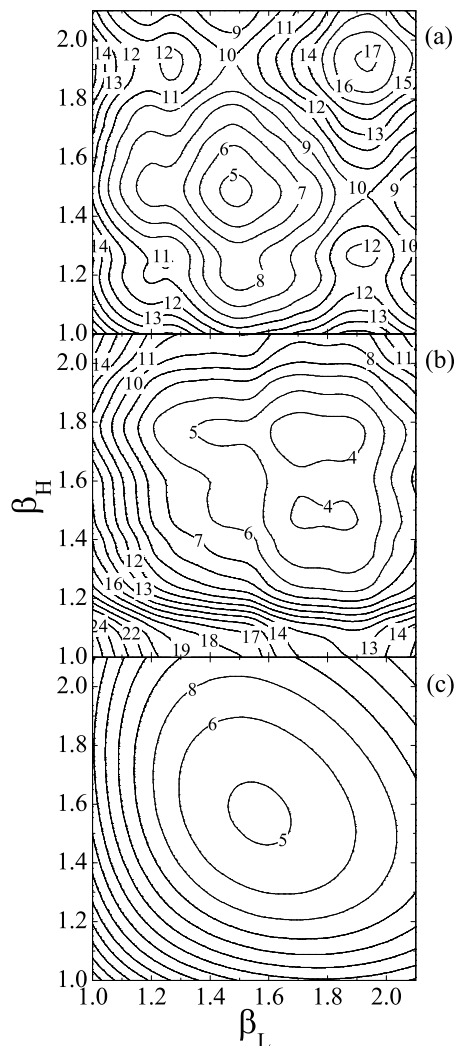


**Figure 2.** Calculated potential energy at the scission point as a function of deformations of the fragments in the binary systems  $^{90}\text{Zr}+^{90}\text{Zr}$  (a) and  $^{76}\text{Se}+^{104}\text{Pd}$  (b). The energy is given in MeV relative to the energy of the fissioning nucleus  $^{180}\text{Hg}$ . For the binary system  $^{90}\text{Zr}+^{90}\text{Zr}$ , the potential energy calculated without shell corrections is shown (c).

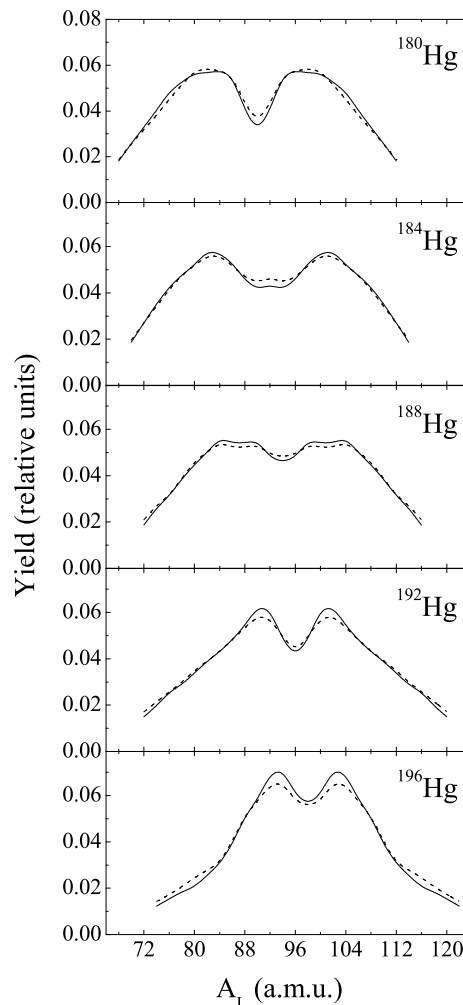


**Figure 3.** Calculated mass distributions of fission fragments for induced fission of  $^{180,184,188,192,196}\text{Hg}$  with the impact energies of 10 MeV (solid lines,  $E_{CN}^*(l=0)=44.2, 43.9, 49.7, 62.4, 56.0$  MeV for  $^{180,184,188,192,196}\text{Hg}$ , respectively) and 30 MeV (dashed lines,  $E_{CN}^*(l=0)=64.2, 63.9, 69.7, 82.4, 76.0$  MeV for  $^{180,184,188,192,196}\text{Hg}$ , respectively) above the corresponding Coulomb barriers for the spherical nuclei.

## References

- [1] Wilkins B D, Steinberg E P and Chasman R R 1976 *Phys. Rev. C* **14** 1832
- [2] Möller P, Madland D G, Sierk A J and Iwamoto A 2001 *Nature* **409** 785
- [3] Gönnerwein F 1991 in *Nuclear Fission Process*, ed C. Wagemans (Boca Raton, FL: CRC Press)
- [4] Hall H L and Hoffman D C 1990 *J. Radiol. Nucl. Chem.* **142** 53
- [5] Oganessian Yu Ts 2007 *J. Phys. G* **34** R165
- [6] Schmidt K-H, Benlliure J and Junghans A R 2001 *Nucl. Phys. A* **693** 169
- [7] Itkis M G, Kondrat'ev N A, Mul'gin S I, Okolovich V N, Rusanov A Yu and Smirenkin G N 1990 *Sov. J. Nucl. Phys.* **52** 601

- Itkis M G, Kondrat'ev N A, Mul'gin S I, Okolovich V N, Rusanov A Yu and Smirenkin G N 1991 *Sov. J. Nucl. Phys.* **53** 757
- [8] Andreyev A N *et al* 2010 *Phys. Rev. Lett.* **105** 252502
- [9] Andreev A V, Adamian G G, Antonenko N V, Ivanova S P and Scheid W 2004 *Eur. Phys. J. A* **22** 51  
Andreev A V, Adamian G G, Antonenko N V and Ivanova S P 2005 *Eur. Phys. J. A* **26** 327
- [10] Andreev A V, Adamian G G, Antonenko N V, Kuklin S N, Ivanova S P and Scheid W 2006 *Eur. Phys. J. A* **30** 579
- [11] Maruhn J and Greiner W 1972 *Z. Physik* **251** 431
- [12] Adamian G G, Antonenko N V, Jolos R V, Ivanova S P and Melnikova O I 1996 *Int. J. Mod. Phys. E* **5** 191
- [13] Raman S, Nestor JR C W, Tikkanen P 2001 *At. Data and Nucl. Data Tables* **78** 1